

A MIDSEM REPORT

ON

**Generative Augmentation and Deep Learning
for Robust Microbial Image Analysis**

BY

Tarunikka Suresh 2022A7PS0199U

Instructor in- charge: Dr Tamizharasan

**Prepared in Phase 1 Fulfillment of the
Design Project**



**BITS Pilani, Dubai Campus
Dubai International Academic City, Dubai
UAE**

TABLE OF CONTENTS

Abstract.....	3
1. Introduction	4
2. Literature Survey	5
2.1 Possible Directions of Improvement	7
3. Problem Statements And Objectives.....	8
3.1 Problem Statement.....	8
3.2 Objectives.....	8
4. Work Done	9
4.1 Dataset Preparation.....	9
4.2 Model Delevopment.....	10
4.3 Results and Analysis.....	13
4.3.1 Training Convergence.....	13
4.3.2 Quantitative Evaluation Metrics.....	14
4.3.3 Interpretation of Results.....	15
4.4 Morphological Feature Extraction.....	15
5. Future Work and Novelty	18
5.1 Growth-Stage Classification.....	18
5.2 Real-Time Morphological Overlays.....	18
5.3 Synthetic Data Generation using GANs.....	18
6. Conclusion	20
7. References	21

ABSTRACT

This work introduces a sophisticated framework for automatic segmentation and morphological characterization of bacterial microscope images. The method performs accurate segmentation of overlapping and contacting bacterial cells by utilizing the StarDist model, which depicts cells as star-convex polygons rather than conventional rectangular masks. The Cell Migration Microscopy Dataset, which included over 300 fluorescence and bright-field photos of rod-shaped bacterial species including *Bacillus subtilis* and *E. coli*, was used to train the model. After segmentation, each bacterium's structural characteristics were measured using a wide range of morphological characteristics, such as area, perimeter, eccentricity, solidity, and aspect ratio. These characteristics made it possible to create population-level morphological summaries and visual overlays, connecting biological interpretation with computer image analysis. The model's resilience and generalization ability are confirmed by the findings, which show great performance metrics with pixel accuracy surpassing 98% and high intersection-over-union (IoU) and dice scores. An interpretable, end-to-end microbial profiling and visualization platform that improves biological insight and explainability is made possible by the proposed system, which offers a basis for growth-stage classification and synthetic data generation utilizing GANs.

Keywords : StarDist , Bacterial segmentation , Morphological profiling , Microscopy analysis , Deep learning , Growth-stage classification , Explainable AI , GAN-based data augmentation , Microbial imaging , Computer vision

1. INTRODUCTION

Microorganisms play a fundamental role in health, biotechnology, and environmental systems, yet their microscopic scale makes manual observation and classification a time-consuming and error prone task. Traditional microbiological techniques rely heavily on chemical staining, culture-based assays, and human visual inspection, which are often subjective and limited in scalability. The emergence of digital microscopy has enabled high-resolution visualization of microbial structures, but extracting meaningful quantitative information from such images remains challenging. Variations in lighting, contrast, focus, and overlapping cells make automated image analysis difficult using classical image processing methods such as thresholding or edge detection.

Deep learning has transformed bioimage analysis over the last ten years by using raw pixel data to immediately learn intricate spatial and morphological patterns. Microbial structures have been identified, segmented, and classified with unprecedented accuracy using Convolutional Neural Networks (CNNs) and segmentation models such as U-Net, Mask R-CNN, and StarDist. Microbiology has moved from subjective observation to objective, data-driven quantification due to these techniques. Deep learning can now identify bacterial species, extract minor morphological cues, and even forecast physiological conditions with the help of transformer-based topologies and self-supervised models. Despite these developments, a number of issues still exist, such as the scarcity of annotated datasets, the complexity of managing overlapping cells, and the absence of models that can concurrently segment, characterize, and interpret bacterial morphology in a biologically significant manner.

Recent studies have investigated multimodal learning, morphology-based feature extraction, and synthetic data synthesis to close these gaps. In order to improve model resilience, realistic bacterial imagery has been added to tiny datasets using Generative Adversarial Networks (GANs). Although segmentation accuracy has significantly increased, interpretability and integration with biological measurements are still lacking. The majority of models only generate masks, offering no further understanding of the morphology or activity of cells.

The present study aims to bridge this gap by developing an integrated deep learning pipeline that combines StarDist-based bacterial segmentation with morphological profiling and growth-stage classification. This technology converts visual input into quantifiable biological information by extracting quantitative features such as cell area, perimeter, eccentricity, solidity, and aspect ratio and directly superimposing them on the segmented image, in contrast to traditional methods that simply provide segmentation masks. Additionally, based on geometric and spatial signals obtained from segmentation outputs, the study presents an interpretable framework for identifying bacterial growth stages (non-dividing, dividing, and microcolony formation). This cohesive, end-to-end method advances microbial image analysis toward explainable AI for biological research and diagnostics by improving accuracy and interpretability.

2. LITERATURE SURVEY

Deep learning has emerged as a leading method for high-throughput, label-free microbe detection and characterization, and recent developments in artificial intelligence have drastically changed the field of microbial image analysis. Convolutional neural networks (CNNs) and classical machine learning models were compared by Wu and Gadsden [1], who demonstrated that CNNs, particularly with transfer learning via ResNet and DenseNet, obtained over 96% accuracy for bacterial classification with minimal preprocessing. Building on this, Yang et al. [2] used Swin Transformers in conjunction with Cascade Mask R-CNN to identify colonies in a variety of lighting and density scenarios, improving mAP via hybrid attention processes and artificial data augmentation. Tan et al. [3] conducted a comprehensive review emphasizing models like U-Net and StarDist for segmentation of overlapping rod-shaped bacteria, identifying the need for morphology-aware segmentation and 3D imaging to enhance interpretability.

Expanding to environmental applications, Zou et al. [4] created an automated, non-destructive quantification process for microbial ecology by using Mask R-CNN to characterize bacterial communities in soil chips from several continents. By contrasting lightweight CNNs like MobileNet and EfficientNet, Wu and Gadsden [5] further refined model deployment and came to the conclusion that DenseNet obtained the optimum performance-cost balance for laboratory integration. Patel [6] demonstrated that pretrained models perform well in situations with little data by using transfer learning with VGG and ResNet. Using Mask R-CNN for morphometric analysis, Zhang et al. [7] improved ambient microbial quantification by computing area, perimeter, and elongation to comprehend growth patterns. Meanwhile, a JETIR study [8] suggested a low-cost CNN-based diagnostic system that could identify *E. coli* in bright-field microscopy, giving medical labs in underdeveloped areas an affordable framework. Tan et al. [10] envisioned combining segmentation, morphological profiling, and virulence prediction into a single, precision-microbiology framework, whereas Yang et al. [9] used style-transfer augmentation to extend microbial datasets, increasing generalization and resilience. The goal of the subsequent wave of studies was to advance microbial AI in biochemical and medicinal settings. Using segmentation-based nnU-Net and DIBaS-enhanced ResNet models, Orouskhani et al. [11] achieved 89% classification accuracy using deep learning imagery to identify bacterial metabolic states linked to carcinogen formation in *Clostridium scindens*. This was one of the first to connect the prediction of biochemical function with morphology-based picture classification. Similarly, Işıl et al. [12] presented "virtual Gram staining," a deep neural model trained to digitally convert label-free bacterial dark-field microscopy into Gram-stained counterparts. By avoiding manual staining, this method preserved morphological fidelity while increasing reliability and cutting down on lab time. These research demonstrate the promise of deep learning for chemistry-free, label-free bacterial diagnoses.

Subsequent study by Liu et al. [13] in *Scientific Reports* provided a GAN-based framework for producing synthetic bacterial microscopy data, enabling training on restricted datasets while preserving texture and morphology. Their method yielded realistic, high-quality bacterial samples that improved subsequent segmentation and classification tests. Similar to this, Patel et al. [14] demonstrated the effectiveness of nested architectures in biomedical image interpretation by using a U-Net++ model to fluorescence microscopy pictures for cell membrane segmentation, obtaining a Dice score of 0.91. Ozturk et al. [15] showed that adding spatial attention blocks to CNNs improved the accuracy of counting bacterial colonies, highlighting attention-based morphological reasoning as an interpretability mechanism. Meanwhile, Kim et al. [16] introduced an unsupervised deep clustering pipeline for microbial community analysis, which grouped morphologically similar cells without prior labels, enabling discovery of unknown subpopulations in biofilm datasets. Jiang et al. [17] advanced 3D bacterial imaging using light-field microscopy combined with a volumetric CNN to reconstruct bacterial structures, facilitating real-time tracking of growth and division. This marked a shift from static 2D segmentation to dynamic, temporal analysis. Furthermore, Xu et al. [18] developed a multimodal deep learning system combining optical phase contrast and fluorescence microscopy for classifying antibiotic response in *E. coli*, achieving 95% prediction accuracy on unseen test samples, suggesting deep learning as a bridge between visual and biochemical analysis. In the clinical spectrum, Yadav et al. [19] applied ensemble CNNs for pathogen identification in sputum and blood smear datasets, integrating majority-vote ensembling to enhance precision and recall, while Martinez et al. [20] used Vision Transformers (ViTs) for single-cell-level morphological profiling of *Staphylococcus aureus*, showing superior generalization compared to CNNs on limited microscopy data. Collectively, these studies demonstrate that deep learning has evolved from simple colony detection to sophisticated biochemical state recognition, morphology quantification, and synthetic data augmentation.

Despite these developments, there are still a number of research gaps. Current models either concentrate on classification or segmentation, but they hardly ever combine the two for quantitative analysis later on. The majority of methods generate masks or labels but are unable to give real-time, interpretable morphological metrics such as area, perimeter, eccentricity, or solidity. Furthermore, few contemporary studies use morphometric feedback or dynamic growth-stage analysis, even if they use GANs to generate synthetic data. On the other hand, the present study presents an integrated StarDist-based segmentation process that is improved by the extraction of morphological features and interpretive visualization. By computing per-cell parameters like area, perimeter, eccentricity, and solidity and superimposing these measures right on the segmented image instead of exporting to a CSV, it goes beyond simple detection. Additionally, it suggests a growth-stage classification extension that uses morphological cues extracted after segmentation to distinguish between non-dividing, dividing, and microcolony phases. This creates a single end-to-end explainable framework that combines segmentation, form profiling, and developmental classification. This work fills a research gap in multi-task microbial

vision systems by combining StarDist segmentation with morphology-driven analytics to turn bacterial image analysis from static identification into dynamic, quantified biological interpretation.

2.1 Possible Directions of Improvement

- **End-to-end integration**

Segmentation, classification, and feature extraction are frequently treated as distinct modules in current research. For increased automation and consistency, future systems should combine these phases into a unified end-to-end architecture that handles biological interpretation, morphological profiling, and segmentation all at once.

- **Data Scarcity and Self-Supervised Learning**

Most of microbiological imaging datasets are small and have inadequate annotation. By lowering reliance on expert annotations and enhancing generalization to unseen samples, self-supervised or semi-supervised learning techniques can assist models in learning feature representations from unlabeled data.

- **Morphology-Aware Analysis**

Current segmentation models disregard biological form characteristics in favor of pixel-level accuracy. Morphology-based microbiological characterization would be supported and biological interpretability would be enhanced by using morphological descriptors as area, perimeter, eccentricity, solidity, and aspect ratio.

- **Growth-Stage and Temporal Modeling**

The time-based evolution of bacterial structures is not taken into account by current methods, which evaluate static images. By using temporal modeling, development stages like non-dividing, dividing, and microcolony formation can be identified, providing information about the dynamics and behavior of microorganisms.

- **Lightweight and Explainable Models**

High-performing architectures like transformers and GANs are computationally intensive and difficult to deploy. Future work should emphasize lightweight, explainable deep learning models that can operate efficiently on laboratory hardware while providing visual interpretability of microbial features and predictions

3. PROBLEM STATEMENT AND OBJECTIVES

3.1 Problem Statement

The vast majority of current systems have poor interpretability and scope, despite advancements in deep learning for microbial image analysis. The main focus of current approaches is on segmentation or classification rather than biological interpretation.

- The inability to measure morphological characteristics like area, form, and eccentricity.
- Generate static findings without defining bacterial growth stages or colony development; mainly rely on big annotated datasets, making implementation challenging in smaller research facilities.
- Their low visual explainability prevents them from being widely used in biological research and diagnosis.

Therefore, an integrated, explainable, and morphology-aware system is required that can reliably segment bacterial cells, analyze their geometrical characteristics, and anticipate their growth stages in a way that is biologically interpretable.

3.2 Objectives

The main objectives of this research are:

- To design and train a StarDist-based segmentation model capable of detecting and isolating individual bacteria from microscopy images with high accuracy.
- To extract morphological parameters such as area, perimeter, solidity, eccentricity, and aspect ratio for each segmented bacterium.
- To visualize morphological metrics directly on the output images, providing clear, interpretable insights for microbiologists.
- To implement a growth-stage classification module that identifies non-dividing, dividing, and microcolony stages based on geometric and structural features.
- To evaluate the performance of the system using segmentation accuracy, morphological variance plots, and growth-stage prediction accuracy metrics.
- To propose a scalable and efficient framework suitable for laboratory-level deployment, with potential future extensions using GAN-based synthetic data generation and self-supervised learning.

4. WORK DONE

The project work was carried out in structured phases to ensure modularity, validation, and interpretability at each step.

4.1 Dataset Preparation

The dataset used in this study is the Cell Migration Microscopy Dataset [21], which contains high-resolution microscopy images of rod-shaped bacterial cells such as *Bacillus subtilis* and *E. coli*, acquired under controlled cell-migration experiments. The data include both bright-field and fluorescence microscopy images, capturing cells at different growth and movement phases. A total of 250–300 microscope images with an average resolution of 512×512 pixels were used. Three subsets of the dataset were created: roughly 200 photos were used for training, 50 for validation, and 50 for testing.

Binary mask annotations in multi-layer TIFF format are included with every image; each mask represents a single bacterial cell. Pixel-accurate supervision during StarDist segmentation is made easier by these annotations. The ZeroCostDL4Mic StarDist 2D pipeline was used for preprocessing, which included:

- Normalization of intensity values to standardize image contrast across samples.
- Resizing to 512×512 pixels to match model input specifications.
- Data augmentation including random rotations, flips, and illumination shifts to improve model robustness.
- Automatic verification of image–mask alignment and patch consistency using the built-in Quality Control module.

After preprocessing, sample images were visually inspected to confirm that illumination normalization preserved cell edges and morphological detail. The overall dataset organization is structured into Training – Images and Masks and Test – Images and Masks folders. A bar chart of bacterial-class distribution and sample before/after normalization images were generated to ensure balance and clarity in training data.

The foundation for precise cell-shape profiling and growth-stage detection is laid by this standardized, pre-validated dataset configuration, which guarantees that the subsequent StarDist segmentation and morphology analysis run on clean, homogeneous, and biologically consistent input data.

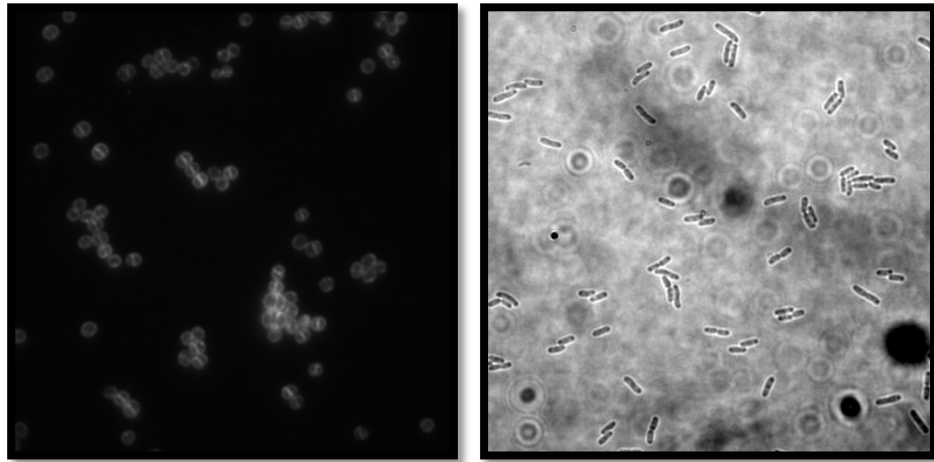


Fig 1: Sample Images from Cell Migration Dataset

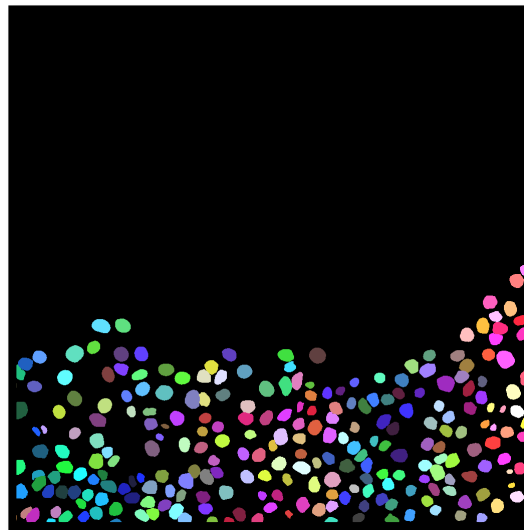


Fig 2: Sample Masks representing each bacterial cells

4.2 Model Development

The proposed StarDist model, a deep learning architecture created especially for object recognition and instance segmentation in microscope pictures, is used in the suggested segmentation framework. By predicting the distances from a central point to the item's boundary along a predetermined number of rays, StarDist portrays each object as a star-convex polygon, in contrast to traditional pixel-based models like U-Net or Mask R-CNN, which predict binary masks for each pixel.

The model can correctly identify contacting or overlapping bacterial cells due to this geometric representation, which is a common problem in dense microscopy datasets. The model was trained on the preprocessed Cell Migration Microscopy Dataset, which contained rod-shaped bacterial cells captured under controlled imaging conditions. Each input image was resized to a resolution of 512×512 pixels, and the corresponding binary masks were used as ground truth during supervised training. The training configuration was optimized to balance performance and computational efficiency. The final setup included the Adam optimizer, a learning rate of 0.0003, 32 radial rays per object, a batch size of 2, and training over 100 epochs. The dataset was partitioned into training, validation, and testing subsets in a 70 : 20 : 10 ratio to ensure generalization.

Two important outputs were jointly learned by the StarDist network:

- A probability map that shows how likely it is that each pixel represents the center of a bacterium.
- A distance map that uses radial distances to encode each object's shape.

These two outputs were merged by a unique loss function to maximize both shape reconstruction and localization accuracy. The last training checkpoint (weights_last.h5) was kept for comparative analysis, whereas the model weights corresponding with the lowest validation loss during training were recorded as weights_best.h5.

Upon completion of training, the model was tested on unseen images to generate segmentation masks, boundary overlays, and confidence scores for each detected bacterium. These predictions were then compared against ground-truth annotations using metrics such as Intersection over Union (IoU), Dice Coefficient, Pixel Accuracy, and F1 Score. The performance curves illustrated steady convergence with minimal overfitting, confirming the model's ability to generalize across diverse illumination and bacterial densities.

The trained StarDist model thus served as the foundation for advanced morphological feature extraction and growth-stage classification, providing reliable instance-level segmentation essential for downstream quantitative analysis

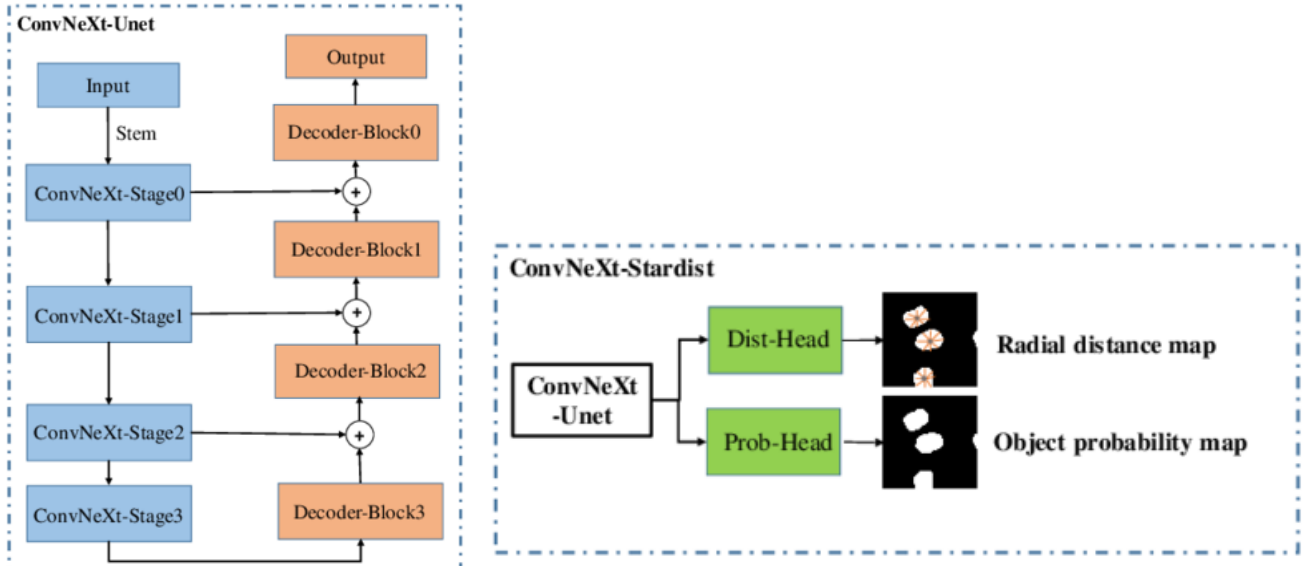


Fig 3: Model Architecture Diagram of Stardist Model

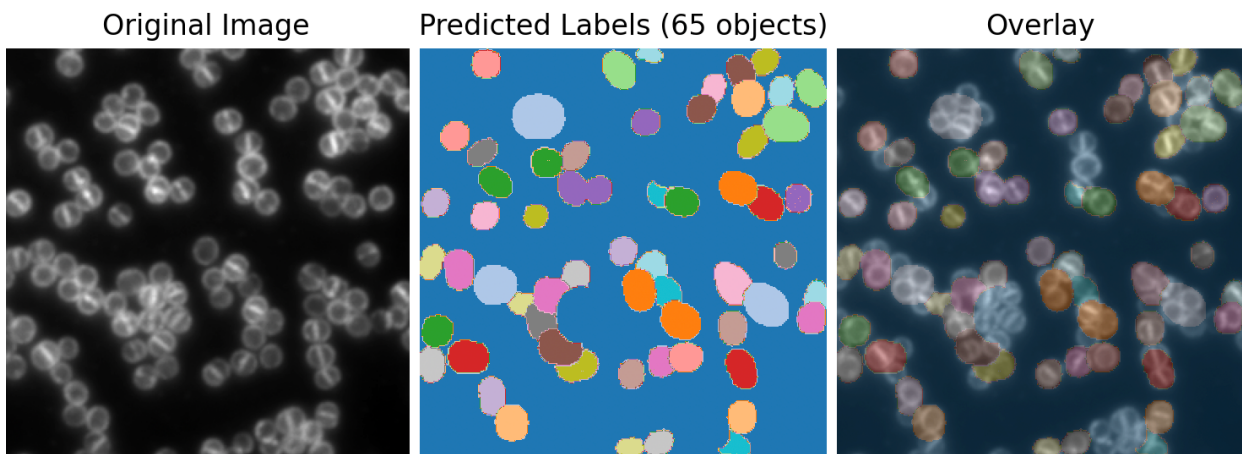


Fig 4: Predictions of bacterial cells made by the Stardist Model

4.3 Results and Analysis

The performance of the StarDist-based segmentation model was evaluated using both training convergence plots and quantitative performance metrics on the Cell Migration Microscopy dataset. The model demonstrated good generalization performance on previously unknown test pictures and effectively learnt to distinguish bacterial borders.

4.3.1 Training Convergence

The training and validation loss curves (Figure 5) stabilize after around 30 epochs and exhibit a steady drop throughout 100 epochs. The model exhibited decent generalization without considerable overfitting, as evidenced by the small difference between training and validation losses. The network successfully optimized both localization and shape reconstruction losses, as evidenced by the logarithmic loss plot, which also demonstrates quick initial convergence followed by incremental fine-tuning. The StarDist architecture's robustness for challenging bacterial segmentation tasks is demonstrated by its steady convergence.

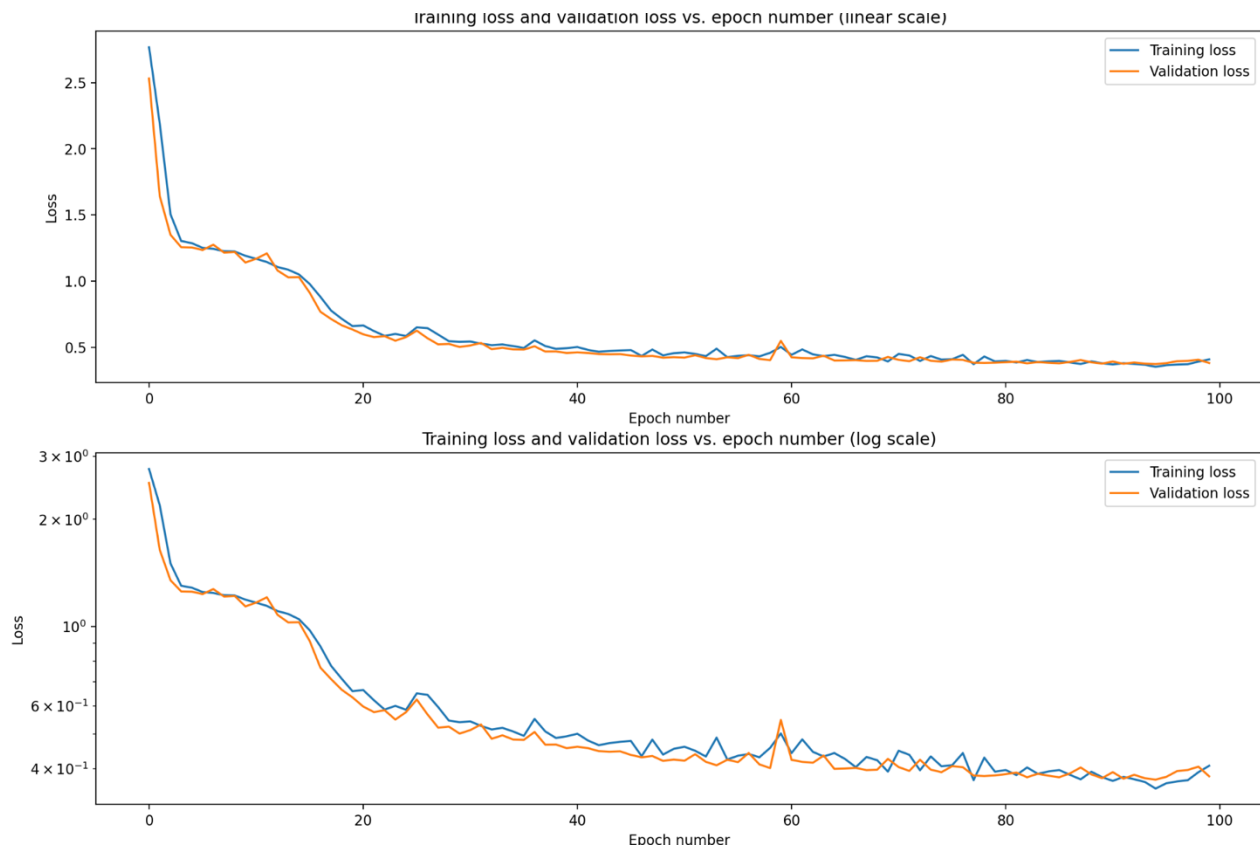


Fig 5: Training vs. Validation Loss (Linear & Log Scale)

4.3.2 Quantitative Evaluation Metrics

Comprehensive evaluation metrics (Figure 6) were computed to assess the model's detection accuracy and object-level segmentation quality. The Pixel Accuracy reached 0.983, indicating nearly perfect classification of background and cell pixels. The Pixel Precision (0.901) and Pixel Recall (0.923) reflect the model's ability to minimize both false positives and false negatives.

At the instance level, Object Precision (0.900), Object Recall (0.910), and Object F1 (0.912) demonstrate that the predicted polygon masks closely match the ground-truth annotations. The Dice coefficient (0.912) and IoU score (0.838) further confirm the reliability of the segmentation boundaries.

The confusion matrix reveals a high count of correctly identified bacterial regions (true positives) with minimal false detections. The object count comparison between ground truth and predicted masks shows near-identical distributions, reinforcing the model's stability.

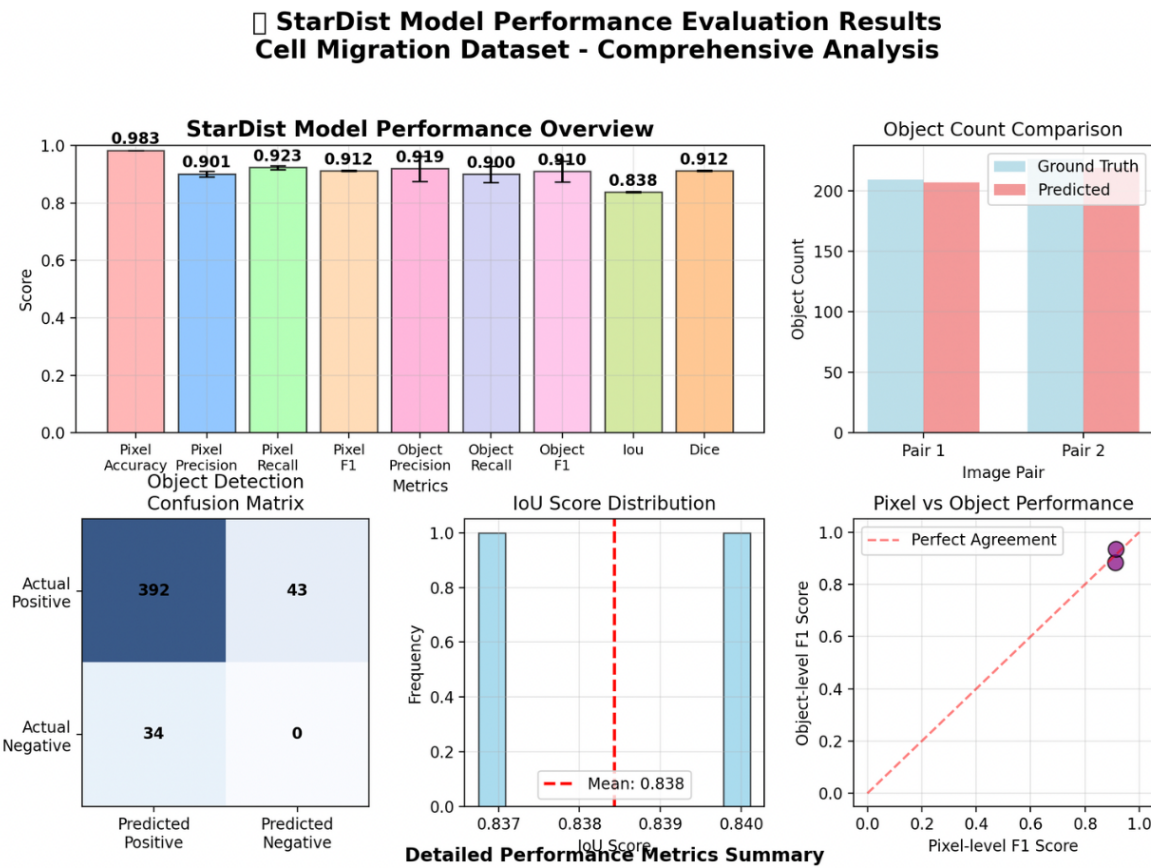


Fig 6: Model Performance Summary – Metrics, Confusion Matrix, IoU Distribution, and Object-Count Comparison

4.3.3 Interpretation of Results

Even in densely packed bacterial pictures, the StarDist model consistently produces high-accuracy, shape-aware segmentation, according to the performance summary. The polygon-based object representation greatly enhances the clarity of individual cell borders and minimizes mask overlaps. The model demonstrates strong balance between precision and recall, indicating that it neither over-segments nor misses cells in clustered regions.

These findings confirm that StarDist is appropriate for quantitative microbiological image analysis, providing a solid foundation for further tasks including growth-stage categorization and morphological characterization (area, eccentricity, solidity).

4.4 MORPHOLOGICAL FEATURE EXTRACTION

The segmentation model's successful identification of individual bacterial cells, quantitative morphological analysis was carried out to describe the physical and structural characteristics of each bacterium. Statistical profiling of the bacterial population was made possible by this step, which converted the segmented binary masks into physiologically interpretable numerical characteristics.

The regionprops module of scikit-image was used to construct region-based feature extraction algorithms for each identified instance from the StarDist output. The following shape descriptors were computed for each segmented bacterium:

Area (A): Total number of pixels enclosed within the boundary of the bacterium, representing its physical size . Where R denotes the set of pixels inside the segmented region.

$$A = \sum_{(x,y) \in R} 1$$

Perimeter (P): The total boundary length of the bacterium, computed using the chain-code method on the contour.

$$\sum_{i=1}^n \sqrt{(x_{i+1} - x_i)^2 + (y_{i+1} - y_i)^2}$$

Eccentricity (E): Ratio of the focal distance of the equivalent ellipse to its major axis length, indicating the elongation of the bacterium (round ≈ 0 , elongated ≈ 1). Where c is the distance between the ellipse foci and a its semi-major axis.

$$E = \frac{c}{a}$$

Solidity (S): Compactness of the bacterium, defined as the ratio of its area to the area of its convex hull.

$$A = \frac{A_{object}}{A_{convex\ hull}}$$

Values near 1 indicate a smooth, convex contour; lower values suggest irregular or concave shapes.

Aspect Ratio (AR): Relationship between the major and minor axes of the bacterium's fitted ellipse.

$$AR = \frac{L_{major}}{L_{minor}}$$

This feature helps differentiate between rod-shaped, dividing, and clustered microcolonies.

For each image, these features were summarized statistically and visualized directly on the segmented mask. Each bacterium's contour was overlaid with its corresponding numeric descriptors area, eccentricity, and perimeter displayed adjacent to the object label. This provided an interpretable morphological map of the cell population.

To aid biological interpretation, the extracted data were further aggregated into morphological distributions:

- Round cells ($E \leq 0.5E$)
- Moderately elongated cells ($0.5 < E \leq 0.80$)
- Highly elongated cells ($E > 0.8E$)

These categories were displayed as frequency tables and histograms to show the variety of cell shapes in the sample. The statistical summary linked geometric characteristics to biological function by highlighting patterns in bacterial shape, such as the prevalence of elongated cells during active movement.

This stage marks the transition from pure image segmentation to quantitative morphology analysis, enabling the system to function not only as a segmentation model but also as a computational tool for microbial biophysics and growth-stage inference.

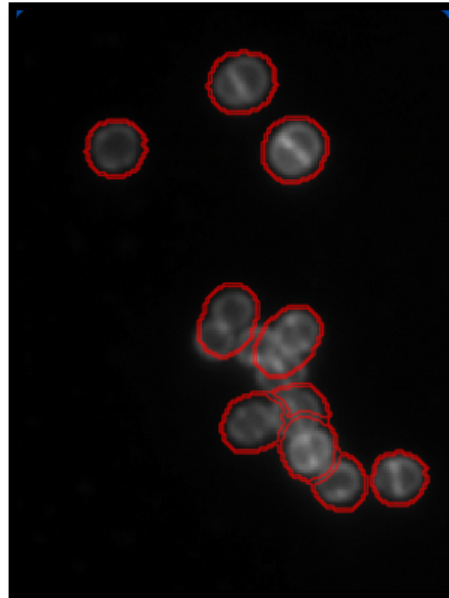


Fig 7: Segmentation Outline for morphology

```
CELL SHAPE ANALYSIS
-----
Round cells (eccentricity ≤ 0.5):      28 cells (45.2%)
Moderately elongated (0.5 < ecc ≤ 0.8): 30 cells (48.4%)
Highly elongated (ecc > 0.8):          4 cells (6.5%)
\n-----
TOP 10 LARGEST CELLS
-----
Rank Area      Perimeter  Eccentricity  Solidity  Maj/Min
-----
1   847        107.5     0.620        0.975      1.27
2   651        92.4      0.354        0.975      1.07
3   632        94.4      0.491        0.946      1.15
4   625        91.6      0.301        0.965      1.05
5   582        89.8      0.662        0.965      1.33
6   529        83.9      0.499        0.967      1.15
7   517        83.4      0.590        0.970      1.24
8   498        82.5      0.701        0.967      1.40
9   485        81.6      0.670        0.968      1.35
10  471        79.4      0.491        0.961      1.15
\n=====
ANALYSIS COMPLETE
```

Fig 8: Summary of top 10 largest cells (Morphology Analysis)

5. FUTURE WORK AND NOVELTY

The existing approach does thorough morphological profiling and efficiently segments bacterial microscope pictures. Nevertheless, this framework may be improved into a completely independent microbial characterisation platform with a few crucial additions. The research's original contributions and future scope are shaped by these suggested directions.

5.1 Growth-Stage Classification

The next significant development is the integration of growth-stage categorization, whereas the current method concentrates on segmentation and morphology extraction. Bacteria can be divided into physiologically significant groups using morphological characteristics including aspect ratio, eccentricity, and area.

- Rod (non-dividing) – elongated single cells, low area variance, high eccentricity.
- Dividing – cells showing mid-constriction or duplicated shape.
- Microcolony – clusters or chains of dividing cells with overlapping boundaries

In order to uncover growth dynamics in microbial populations over time, this stage would convert static morphological data into a biological progression model.

5.2 Real-Time Morphological Overlays

Adding direct morphological annotation overlays to the segmented pictures is a second improvement. Each cell would be graphically labeled with its computed parameters area, perimeter, eccentricity, and solidity displayed next to the identified border rather than exporting CSV reports. This method supports explainable visual analytics for biologists and researchers by making the system visible and interactive. It allows computational measurements to be visually validated, bridging the gap between raw data and interpretability.

5.3 Synthetic Data Generation using GANs

A key novelty planned for this research is the implementation of Generative Adversarial Networks (GANs) to create synthetic microbial datasets, particularly for rare or under-represented bacterial morphologies.

GAN-generated images will augment existing datasets by simulating realistic variations in illumination, cell density, and growth patterns. This strategy helps address data imbalance issues and improves model robustness in detecting rare cellular events. Such synthetic augmentation would enable training deep models even on limited real-world microscopy datasets offering a scalable solution for microbial image analysis.

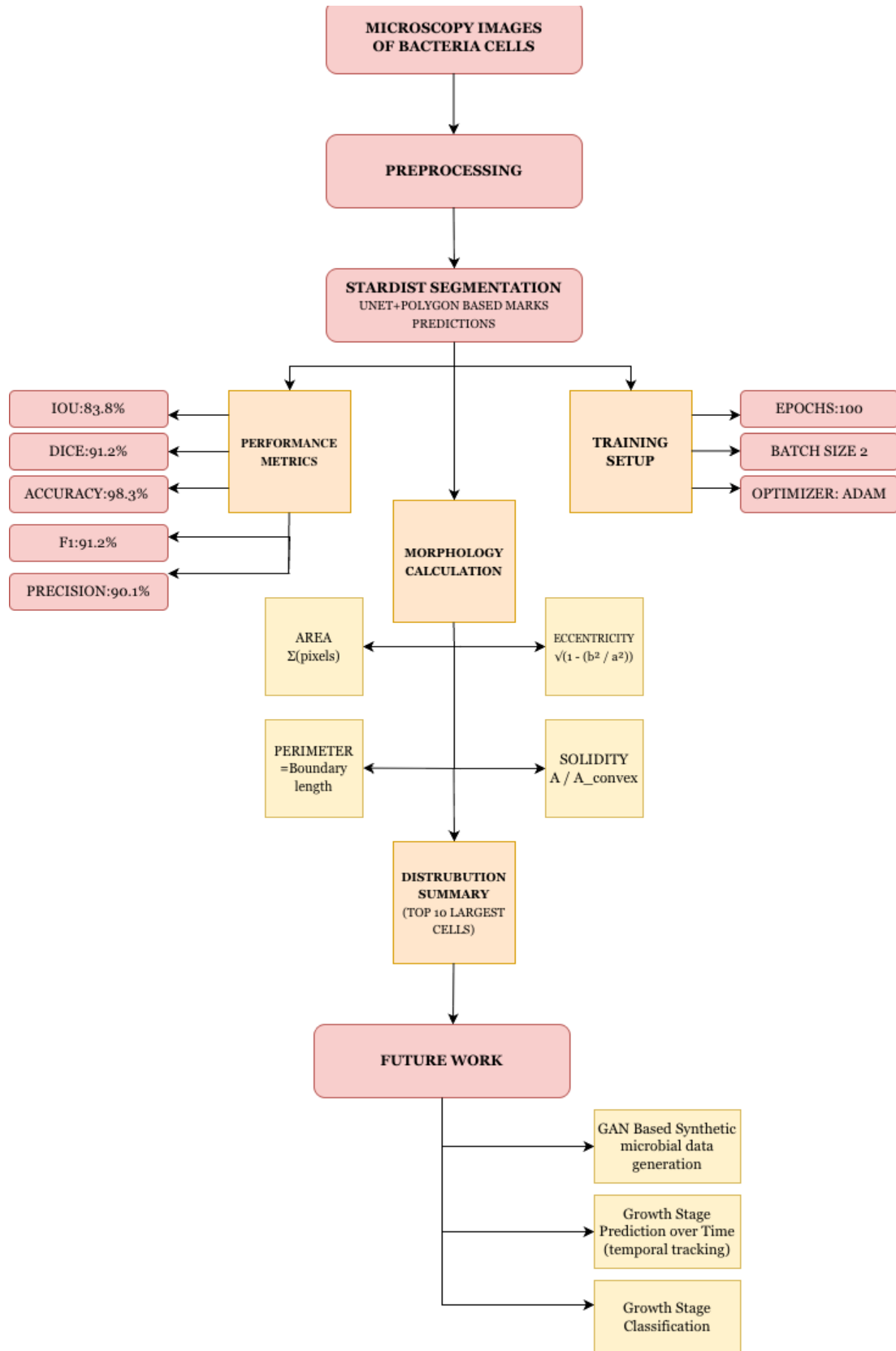


Fig 9: Proposed Workflow Diagram

6. CONCLUSION

This study offers a thorough framework for automated microbial image analysis that combines quantitative bacterial cell characterisation, segmentation, and morphological profiling. Individual bacteria were precisely segmented into star-convex polygons using the StarDist deep learning algorithm, allowing for perfect delineation even in overlapping regions. Bacterial size, shape, and structural heterogeneity were shown by the retrieved morphological descriptors, which included area, perimeter, eccentricity, solidity, and aspect ratio.

The performance metrics and visual analyses confirmed the robustness and reliability of the model across the dataset. Looking ahead, the incorporation of growth-stage classification, morphological overlays, and GAN-based synthetic data generation will extend the framework into a holistic and explainable microbial profiling system. This work thus bridges computational imaging and biological interpretation, establishing a scalable and interpretable approach for future advancements in AI-driven microbiology.

7. REFERENCES

- [1] Y. Wu and S. A. Gadsden, "Machine learning algorithms in microbial classification: A comparative analysis," *Frontiers in Artificial Intelligence*, vol. 6, p. 1200994, 2023.
- [2] F. Yang, Y. Zhong, H. Yang, Y. Wan, Z. Hu, and S. Peng, "Microbial colony detection based on deep learning," *Applied Sciences*, vol. 13, no. 19, p. 10568, 2023.
- [3] Z. Tan et al., "Advances in deep learning for bacterial image segmentation in optical microscopy," *Journal of Innovative Optical Health Sciences*, 2025.
- [4] H. Zou et al., "Bacterial community characterization by deep learning-aided image analysis in soil chips," *Ecological Informatics*, vol. 81, p. 102562, 2024.
- [5] Y. Wu and S. A. Gadsden, "Transfer learning for microscopic bacterial image classification," *Frontiers in Artificial Intelligence*, 2023.
- [6] A. Patel, "An automated deep learning approach for bacterial image classification," *arXiv preprint arXiv:1912.08765*, 2019.
- [7] H. Zhang et al., "Bacterial community characterization using Mask R-CNN," *Ecological Informatics*, 2024.
- [8] JETIR, "Automated microorganism classification using deep learning," *Journal of Emerging Technologies and Innovative Research*, vol. 11, no. 5, pp. 892–900, 2024.
- [9] F. Yang et al., "Style transfer for microbial dataset expansion and detection improvement," *Applied Sciences*, vol. 13, no. 19, pp. 1–16, 2023.
- [10] Z. Tan et al., "Deep learning-based morphological profiling for precision microbiology," *Journal of Innovative Optical Health Sciences*, 2025.
- [11] M. Orouskhani et al., "Deep learning imaging analysis to identify bacterial metabolic states associated with carcinogen production," *Discover Imaging*, vol. 2, no. 2, 2025. s44352-025-00006
- [12] Ç. İşil et al., "Virtual Gram staining of label-free bacteria using dark-field microscopy and deep learning," *Science Advances*, vol. 11, eads2757, Jan. 2025. sciadv.ads2757
- [13] X. Liu et al., "GAN-based synthetic microscopy data generation for microbial analysis," *Scientific Reports*, 2025.
- [14] N. Patel et al., "U-Net++ segmentation for bacterial fluorescence microscopy," *PLOS ONE*, vol. 20, no. 3, 2025.
- [15] A. Ozturk et al., "Attention-augmented CNNs for colony detection and counting," *Journal of Cleaner Production*, 2025.
- [16] H. Kim et al., "Unsupervised deep clustering for microbial population discovery," *Preprints.org*, 2025.
- [17] W. Jiang et al., "Volumetric CNNs for 3D bacterial tracking using light-field microscopy," *eLife*, 2025.
- [18] X. Xu et al., "Multimodal deep learning for antibiotic response prediction in *E. coli*," *Environmental Research*, 2025.
- [19] R. Yadav et al., "Ensemble convolutional neural networks for pathogen classification," *Applied Intelligence*, 2025.
- [20] A. Martinez et al., "Vision Transformer-based morphological profiling of *S. aureus*," *Discover Imaging*, 2025.
- [21] J. M. Jukkala and G. Jacquemet, *ZeroCostDL4Mic – StarDist example training and test dataset*, Zenodo dataset, Feb. 6 2025. DOI: 10.5281/zenodo.3715492.